AIP | Physics of Plasmas

Effective post-acceleration of ion bunches in foils irradiated by ultra-intense laser pulses

A. A. Andreev, P. V. Nickles, and K. Yu Platonov

Citation: Physics of Plasmas (1994-present) **21**, 083110 (2014); doi: 10.1063/1.4892957
View online: http://dx.doi.org/10.1063/1.4892957
View Table of Contents: http://scitation.aip.org/content/aip/journal/pop/21/8?ver=pdfcov
Published by the AIP Publishing

Effective post-acceleration of ion bunches in foils irradiated by ultra-intense laser pulses

A. A. Andreev,[1,2,3] P. V. Nickles,[1,4] and K. Yu Platonov[5]
[1]*Max Born Institute, Max Born Str. 2a, D-12489 Berlin, Germany*
[2]*Saint Petersburg State University, University Emb. 7-9, 199034 Saint Petersburg, Russia*
[3]*ELI-ALPS, Dugonics ter. 13 H-6720 Szeged, Hungary*
[4]*Center of Relativistic Laser Science, Institute for Basic Science, Gwangju 500-712, South Korea*
[5]*Saint Petersburg State Technical University, Politekhnicheskaja 29, 195251 Saint Petersburg, Russia*

(Received 24 May 2014; accepted 30 July 2014; published online 14 August 2014)

Two-step laser acceleration of protons with two foils and two laser pulses is modelled and optimized. It is shown that a nearly mono-energetic distribution of proton bunches can be realized by a suitable parameter choice. Two-step acceleration schemes make it possible to obtain both higher efficiency and energy as compared to the acceleration with only one laser pulse of an energy equal to the sum of the energy of the two pulses. With the aid of our analytical model, the optimal distance between the two targets, the delay between the two laser pulses, and the parameters of the laser pulses are determined. Estimates and results of the modelling are proven with 2D PIC simulations of the acceleration of proton bunches moving through the second target. © *2014 AIP Publishing LLC*. [http://dx.doi.org/10.1063/1.4892957]

INTRODUCTION

Lasers of the PW class have reached maximal proton energies of about 80 MeV.[1] However, this value is still too low for several applications, specifically when the treatment of cancerous diseases[2] is the purpose. A further enhancement of the proton energy by an increase of the laser intensity is very costly and diminishes the competitiveness of such laser accelerators in comparison with classical sources. In the latter, the acceleration takes place in several simple cycles and therefore some papers reported attempts to find analogous "cascaded" variants with lasers. However, in simulations[3,4] and in preliminary experiments,[5,6] only a very small acceleration was achieved, accompanied by a modification of the energy distribution that is inappropriate for use in such a cyclic accelerator. In the paper,[6] it was shown experimentally that a dip and neighbouring peaks in the distribution function of the energetic protons can appear, if such a bunch is propagating through a thin foil irradiated by an intense laser pulse. Unfortunately, the relative amount of the accelerated protons in the experiment[5,6] (passing from the dip into the peak) was very low as compared to the total number of protons in the complete distribution function.

In the present work, there are investigated both the possibility of an additional acceleration and the modification of the distribution function of the accelerated ions using a scheme with two targets (Nos. 1 and 2) separated by a given distance l_1 (see Fig. 1) and irradiated with two ultra-intense laser pulses at a given delay time. The first laser pulse irradiates the front surface of the first targets and the second pulse hits one of the surfaces of the second target. In such a scheme, the first target is the source of protons with a specific energy range (characteristic energy is in the MeV range and the distribution can be very broad as well as quasi-mono-energetic). A broad energetic distribution takes place if protons are distributed in a layer of tens of nm thickness (due to adsorption of water vapor) or if the target is of hydrogen-consisting materials (plastics). In order to obtain a quasimonoenergetic distribution, one needs specifically shaped targets.[10,14] For example, ultrathin hydrogen-consisting layers (several nm thick) on the target rear surface or ultrathin foils in combination with circularly polarized laser light in the so called radiation pressure acceleration regime (RPA) have been proposed (see Ref. 9). A proton bunch accelerated at the rear surface of the first target propagates to the second target in the positive direction on the x-axis and becomes broadened in the space between the two targets according to its energy distribution. The spatial broadening of the bunch is thereby proportional to the distance between the two targets l_1. The second target is irradiated by a second laser pulse during the transmission of the proton bunch through it. The second laser pulse can be also a split-off and delayed part of the first pulse.

A strong ambipolar field is created on the surface of the second target at a distance of the order of the Debye radius, which is directed from the target surface into vacuum and has different signs at the two surfaces of the target. This field exists only during the lifetime of the hot electrons in the target and its spatial-temporal parameters depend on the kind of

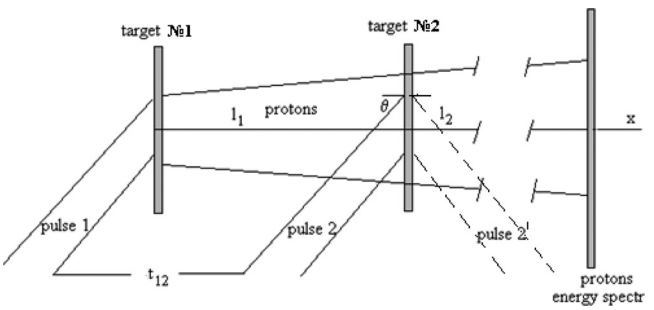

FIG. 1. Scheme of a two-cascaded laser accelerator of protons.

target and on which target surface is irradiated. An enhancement of the thickness of the second target results in an asymmetry of the ambipolar field, but a laser pre-pulse can also cause an asymmetric field. In this way, with the choice of the target structure, the laser pulse profile and which target surface is irradiated, one can accelerate protons in a field with a duration of several hundreds of femtoseconds (for limited targets). During the lifetime of the field not all of the protons in the bunch can interact with it. As a result, for a second target with a thickness in the micron range, a slowing down at the front surface and acceleration at the rear side takes place for different groups of protons, differing in energy and space. For example, protons slowed down at the front side may arrive in the region of the accelerating field at the rear side after a time that is sufficient for a relaxation of the field, and therefore they will not be further accelerated. In consequence of such temporal dynamics, the front and tail of the distribution function of the proton energy are unchanged, whereas the central part of the distribution is deformed. Specifically, protons moving into the range of the accelerating field can catch up to those propagating in front of them. After that, the field disappears and the remaining protons with lower energy maintain their energetic distribution. That causes the distribution function to acquire a dip and a peak. Their configuration and position depend on the distance between the targets, the proton energy, and the delay of the second laser pulse.

The aim of our investigation is a quantitative description of the resulting proton distribution function and a selection of optimal parameters for the setup that makes possible the formation of a mono-energetic and directed distribution of protons with given energies. In the paper, the required conditions for that are described allowing calculation of the energy of the protons after an additional acceleration in the second target of the two-cascade scheme. The distribution function (solution of the kinetic equation) of the protons, accelerated by the second target is here derived by the method of characteristics. In doing so, it is presumed that the proton bunch has no influence on the electromagnetic field of the second target (probe beam approximation). The condition for this approximation is a low density of the proton bunch to be accelerated. The quantitative limitation of its applicability is given in the Appendix.

SIMULATION OF THE ELECTRIC FIELD STRUCTURE CREATED AT THE SECOND TARGET AND ACCELERATION OF THE PROTONS

In order to show the potential of cascaded proton acceleration according to the scheme given in Fig. 1, 2D PIC simulations have been performed for the interaction of the proton bunch (assumed to be created by the target No. 1) with the target No. 2 irradiated with a laser pulse. A modelling of the experimental situation[6] with two laser pulses and a distance between the two targets of tens of microns is impossible because the time of the motion of the bunch between the two targets (hundreds of ps) is too large for a PIC simulation with a temporal step of tens of femtoseconds. It is here assumed that the proton bunch from the first target has a Gaussian energy distribution with a half width of 10 keV and a central energy of 10 MeV. Such a quasi-monoenergetic bunch can be realized using a ultrathin 5 nm CH foil irradiated with a highly contrasted circularly polarized 45 fs laser pulse with an intensity of 5×10^{19} W/cm^2.[10] The longitudinal and the transversal dimensions of the bunch are chosen to be $0.5\ \mu\text{m} \times 2\ \mu\text{m}$, and it is assumed that the Gaussian profile remains during the whole measurement. In order to take into account a laser prepulse, the second target was of 5 μm thick target from Al^{+6} (as given in Fig. 1) with an ion density of 6 n_{cr}. The thickness of the second target of 5 μm was chosen such that the proton bunch was localized within the second target.

So as to eliminate a retardation of the protons at the front surface of the second target heated by the laser pulse, the initial position of the proton bunch centre was chosen to be in the Al target 1 μm apart from the front side. Such initial position corresponds to a specific temporal delay between the laser pulses. The Gaussian laser pulse (second pulse in Fig. 1) with an intensity of 3.4×10^{19} W/cm^2, a duration of 60 fs, and a diameter of 6 μm irradiates the front side of the Al target 30 fs after the start of the propagation of the proton bunch. During the movement of the bunch to the front surface of the second target (90 fs), the time interval is such that the entire laser pulse can interact with the front surface, creating an ensemble of relativistic (hot) electrons that can overtake the proton bunch and generate the field for the acceleration of the latter. To study the dependence of the acceleration process on the density n_p of the proton bunch, the simulations were performed for both at $n_p = 1.0\ n_{cr}$ and $n_p = 0.05\ n_{cr}$, where n_{cr} is the critical electron density. A similar modelling was reported in Ref. 7, where a situation of a bunch with very low density of $n_p \approx 0.01 n_{cr}$ and with energetic broadening of $\sim$2% was investigated. Results of our simulation of the proton bunch distribution function for two different densities are depicted in Fig. 2(a), whereas Fig. 2(b) shows the transversal field distribution.

As visible in Fig. 2(a), a denser proton bunch has a higher maximal energy, but a broader distribution. This results from the appearance of the electric field at the edge of the proton bunch during its propagation in the target. Such a field has a remarkable value only if proton densities exceed a few tens of percents of the target density. The reason for the appearance of the field is connected with the interaction of the electron shock wave at an enhancement of the ion density at the position of the proton bunch. The built-up ambipolar field slows down electrons and accelerates protons. Retardation of the relativistic electrons in the field results in a small difference in the velocities of the electron and proton bunches. This electric field propagates through the target up to its rear side. Therefore, proton bunches with high density are accelerated in their motion within the target and at their transition through the rear surface as well. In contrast, for low-dense bunches no ambipolar field is generated within the target and their propagation has a clearly defined single-particle character. Such bunches will be accelerated only at their transition through the target surfaces and correspondingly their energy is reduced (see Fig. 2(a)). When the hot electrons are detaching from the target surfaces within a distance of the Debye radius, the acceleration of proton bunches

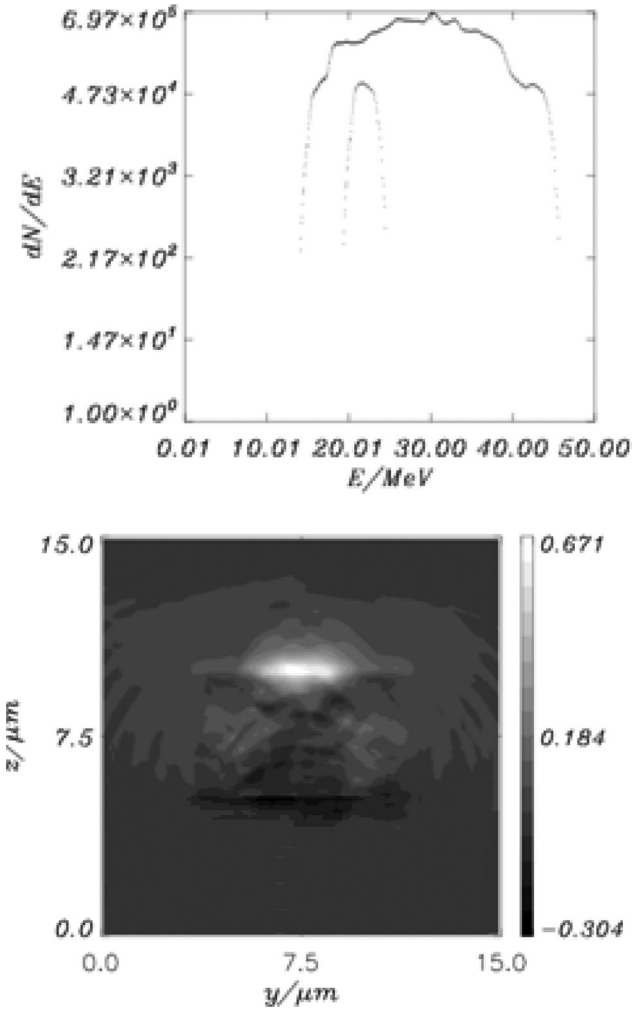

FIG. 2. (a) Distribution functions of protons in accelerating a quasi-monoenergetic proton bunch ($\Delta E = 10$ MeV) of density $n_p = 1.0\ n_{cr}$ (black color) and $n_p = 0.05\ n_{cr}$ (blue color) at the moment 100 fs after start of the second laser pulse irradiation. (b) Spatial distribution of the electric field (in the units of the laser one) at the second target at the moment 90 fs. Intensity of the laser pulse is 3.4×10^{19} W/cm^2 duration 60 fs, focal spot size is 6 μm. Target is a layer of Al^{+6} with thickness of 5 μm and ion density of 6 n_{cr}.

is decreased for any density. Therefore, the maximal proton energy is due to the acceleration length for the dense bunch being considerably higher than for the low-density bunch (Fig. 2(a)). High maximal energy is accompanied by an energy broadening and the monochromaticity of the distribution is completely lost, i.e., $\Delta E/E \sim 1$. A reduction of the proton density (and number) by a factor of 20 diminishes the spectral width ($\Delta E/E \sim 3/20 \approx 15\%$), but also the maximal proton energy is reduced. It is worth noting that a higher-density proton bunch contains also a larger number of protons and, for specific applications, a reduction of the spectra can be performed by a filter, which could cut out the higher-energetic part comprising a proton number comparable to those of the low-density bunch. In the simulation, the thickness of the second target, the initial position of the bunch, and the delay time of the laser pulse were chosen in such a way as to eliminate the influence of the retarding field on the proton bunch at the front side. For the second target with a thickness less than or comparable to the longitudinal size of the bunch, it is impossible to exclude such retarded field action. In order to determine for such cases, the spatio-temporal characteristic of the electrical field we have performed a modelling of the laser plasma of thin targets. For that it was assumed that the target is irradiated under 45° by a p-polarized Gaussian laser pulse with a diameter of 6 μm, a duration of 50 fs and an intensity of 3.4×10^{19} W/cm^2. The 1 μm thick target is of Al^{6+} ions and its rear side is covered with a 100 nm layer of hydrogen. The transversal size of the target of 70 μm has no influence on the field distribution, because at the simulation time of 150 fs, the field in the target centre has nearly disappeared and the cloud of hot electrons will not arrive at the target edges. The target was situated in a box of $50 \times 50\ \mu m^2$, the simulation step was 10 nm and one spatial cell contained 30 quasi-particles. The simulations provided the spatial distribution of the electric field components along the direction of the laser beam (the component normal to the target is $\sqrt{2}$ larger) and gave also the temporal field dynamics.

As shown in Figure 3 is a cross section (at the axis of the laser beam) and the 2D field distribution at the moment near the end of the laser pulse, and also at the moment when the cloud of hot electrons arrives at the boundary of the box.

It was supposed that the laser pulse arrives to the target at 40 fs. Up to 90 fs, there is the reflected laser pulse and the laser field at the target surface differs from the ambipolar one (see Fig. 3). After 90 fs, the electric fields stay constant on the target over the time of the laser period.

The small thickness of the target and the box size does not influence either the cooling speed of the electrons or the relaxation of the ambipolar field up to 160 fs, i.e., the field as visible in Fig. 3 does not arrive the edge of the box. In Fig. 3, it is also shown that the electric field in the centre of the laser spot ($y = 25\ \mu$m) has a remarkable value in the interval 80–130 fs, with the maximum at a time of about 100 fs. After that a shift of the maximal field occurs together with the hot electron cloud along the target surface and a fast field relaxation due to the adiabatic decay of the electron cloud appears. Additionally, also the characteristic size of the field given by the triangles in Figs. 3(a) and 3(b) drops off. Contribution of the exponential "tail" of the density distribution $n_i(z) = n_0 \exp((z - z_0 + l_f/2)/L)\theta(z_0 - l_f/2 - z)$ (where $z_0 = 25$ mkm, $n_0 = 6 \times 10^{22}$ cm^{-3}) with the scale $L = 1\ \mu$m at the front surface reduces (in the simulations) the field amplitude at the front side by about ~5 times as compared with a sharp target edge. Such a density profile makes it possible to reduce or even exclude a slowing-down field, but preserves an accelerating one. For its realization, a prepulse is required, which should have the duration less than the transmission time of a heat wave through the target (~10 ps at an intensity of $\sim 10^{14}$ W/cm^2).

During the action of the laser pulse on thin targets ($l_f \leq 1\ \mu$m), the accelerating and retarding field "triangles" have a comparable amplitude and spatial size (see Fig. 3). "Thin target" means a target with a thickness less than or comparable with the Debye length of the hot electrons with a characteristic "triangular" shape field as in Fig. 3; i.e., of scale ~1 μm. The distance between accelerated and slowed down protons in the regions of the field (triangles in Fig. 3)

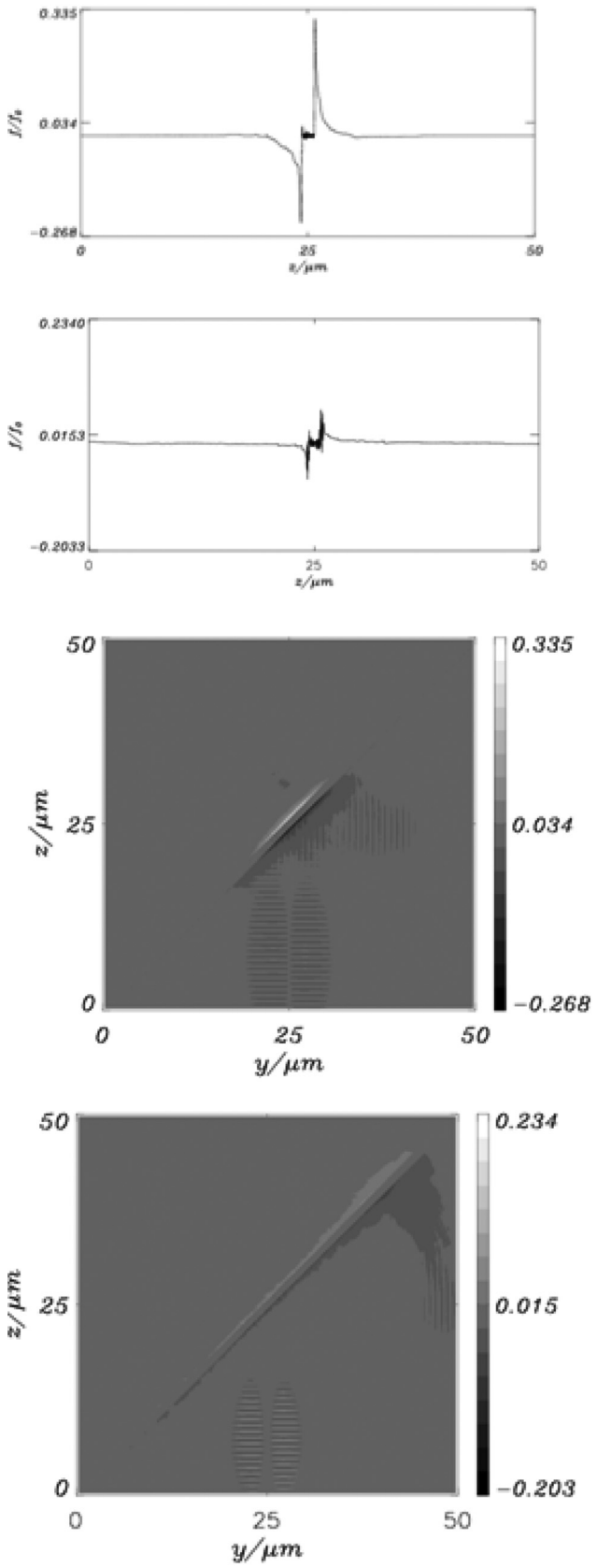

FIG. 3. (a) and (b) Profile of the z-components of the ambipolar field at the centre of the laser beam at the moments 80 fs and 154 fs; (c) and (d) 2D distribution of the z-component in the box at the same moments. All results are averaged over the period of the second laser pulse. Value of the field is given in units of the laser field. Laser pulse with $I_L = 3.4 \times 10^{19}$ W/cm^2, duration 50 fs, irradiated the Al^{+6} target with thickness of 1 μm at the angle of incidence 45°.

is nearly comparable to the foil thickness l_f and the scale of the triangle.

The transition time of MeV-protons through the foil is (in the simulations) nearly equal to the lifetime of the field. Therefore, protons located in the retarding field will not feel the accelerating field and vice versa. Correspondingly, the different intervals in the distribution function are subject to changes under the action of two "triangles" of the field. Changing the target thickness, both intervals can approach each other and create in this way a strong asymmetry between the accelerating and the retarding interval of the field up to a total suppression of the retarding contribution. Limiting the transversal size of the target allows a slowdown of the spatial decay of the electron cloud and its motion along the surface, which results in a remarkable prolongation of the field lifetime. Thus, the simulations show that a considerable acceleration of protons is possible, when using a second target. With a suitable choice of the target parameters, direction of irradiation, and delay time between the laser pulses, one can significantly vary the characteristic of the accelerating field at the target. For further analysis, we have elaborated the analytical model of the processes.

ANALYTICAL MODEL

Now, we consider the dynamics of MeV protons in the "triangular" ambipolar field. It is worth remarking that, at the propagation distance of the protons of millimetres, an electric field of micron size affects only a monochromatic component of the distribution function and the number of protons is small as compared to the total number. The main part of protons will be accelerated at propagation lengths of tens of microns.

Kinematics and dynamics of the proton motion and development of their distribution function

Starting from simulation results of the spatial-temporal parameters of the electrical field, we have shown that the action of each of the triangular fields on the protons can be approximated by a force accumulated in one point with a given lifetime. The condition for that is the short lifetime of the field τ_f as compared to the proton propagation time over the extent of each triangular field (Debye length $r_{De1,2}$), where $\tau_f < r_{De1,2}/\sqrt{2\varepsilon_i/m_p}$.

As visible in Figure 3(a), the scales $r_{De1,2}$ are comparable and in the evaluation they are taken as equal. The expression for the force (taking into account the accelerating and retarding triangular fields) is of the form

$$F(x,t) = U_1(t - t_{12})\delta(x - l_1) + U_2(t - t_{12})\delta(x - l_1 - l_f). \quad (1)$$

Now, we estimate the influence of each of the two products in (1) on the motion of a single proton with an energy ε_i and on the distribution function. A retarding field with the potential U_1 acts on the proton at the moment l_i/v_i and it holds for the function U_1 as: $U_1(l_1/v_i - t_{12})$. The accelerating field acts on the proton in the moment $(l_1 + l_f)/v_i$; thus, the argument of function U_2 is $U_2((l_1 + l_f)/v_i - t_{12})$. The lifetime of

the field is $\tau_f < l_f/v_i$ and therefore only one of the products of the expression (1) acts on the particle with given velocity v_i. The second product interacts with another particle, which has a velocity differing by the amount $v_i l_f/l_i$. At a given distance l_1 between the targets and a fixed delay time $\tau_{1,2}$, the retarding field influences the distribution function of those the protons, which have a velocity in the interval of $v_i \in [(l_1 - r_{De1})/t_{12};\ l_1/t_{12}]$, whereas the accelerating field interacts with the protons having a velocity $v_i \in [(l_1 + l_f)/t_{12};\ (l_1 + l_f + r_{De2})/t_{12}]$. Apparently, the intervals do not overlap each other and an additive action of the two products (1) on different parts of the energy distribution of the protons take place. It is worth noting that in our case l_f and $r_{De1,2}$ are comparable (see Fig. 2(a)), and therefore the velocity intervals of the acceleration and retardation are very close to each other (distance between intervals are of the order of the interval widths). In thick targets $l_f \gg r_{De1,2}$, the intervals can have considerable separation. In the above-discussed model, we have presumed a simultaneous emission of ions with all velocities from the first target and correspondingly the same delay time t_{12} for protons of the whole energy distribution. Such an assumption is fulfilled when the delay time is much longer than the characteristic ion acceleration time $\sim\tau_f$.

At the beginning, we look for the formation of the distribution function under the action of each of the triangular fields, i.e., the force $U(t)\delta(x - l_1)$ and assume that the potential U can be positive as well as negative. After that analysis, we consider a joint action of the two products in formula (1). A change in the potential barrier is connected with heating or cooling the plasma and can be described by the following dependence on time:

$$U(t) = \frac{\pm T_{e2}}{1 + \left((t - t_{12})/\tau_a\right)^n} \quad t < t_{12};$$
$$\frac{\pm T_{e2}}{1 + \left((t - t_{12})/\tau_f\right)^n} \quad t > t_{12}, \tag{2}$$

where $T_{e2} > 0$ is the electron temperature in the second target, signs +/− are related to protons accelerated or retarded by the field. Rise time of the field $\tau_a \approx \tau_L/2$ is much less than the characteristic damping time τ_f (lifetime of the field). The temporal dependence (2) of the height of the potential barrier of the hot electrons at $n = 2$, describes the adiabatic law of the cooling of the hot electron cloud. At the irradiation angle of 45° in addition to the adiabatic cooling, there is also a shift of the hot electron cloud along the surface (Figs. 2(c) and 2(d)), which can cause a much faster decrease in time of the temperature in the centre of the laser pulse spot. The parameter n can be selected from the simulation. It should be noted that $n = 2$ in (2) is not of primary meaning for further results and especially for the proton distribution function. Of more importance is the temporal scale τ_f of the field action in (2). The solution of the equation of proton motion with the force (1) is as follows:

$$\begin{cases} p \equiv G_p(p_0, t) = p_0 & 0 < t < l_1 m_p/p_0 \\ p \equiv G_p(p_0, t) = \sqrt{{p_0}^2 + 2m_p U(l_1 m_p/p_0)} & t > l_1 m_p/p_0. \end{cases}$$

Here, p_0 is the initial proton momentum. For the case of sufficiently long time, one obtains for the solution $f(p)$ of the kinetic equation performed by the method of characteristics

$$f(p) = \int_{-\infty}^{\infty} \delta\left(p - \sqrt{{p_0}^2 + 2m_p U(p_0)}\right) f(p_0)\, dp_0$$
$$= \sum_i f(p_{0i}(p)) \left| \frac{\partial \sqrt{{p_0}^2 + 2m_p U\left(l_1 m_p/p_0\right)}}{\partial p_0} \right|^{-1}_{p_0 = p_{0i}(p)}.$$

Here, $p_{0i}(p)$ are all branches inverse to the function $p(p_0) = \sqrt{{p_0}^2 + 2m_p U(l_1 m_p/p_0)}$. Now, it is convenient to change from the momentum distribution $f(p)dp = f_\varepsilon(\varepsilon)d\varepsilon$ to the energetic distribution $\varepsilon(\varepsilon_0) = \varepsilon_0 + U(\sqrt{m_p} l_1/\sqrt{2\varepsilon_0})$. Taking into account that $d\varepsilon/dp = \sqrt{2\varepsilon/m_p}$, one obtains the final expression for the distribution function of protons that propagated through a part of the field with a given sign

$$f_\varepsilon(\varepsilon) = \sum_i f_\varepsilon(\varepsilon_0) \left| \frac{\partial \varepsilon(\varepsilon_0)}{\partial \varepsilon_0} \right|^{-1} \Bigg|_{\varepsilon_0 = \varepsilon_{0i}(\varepsilon)}. \tag{3}$$

Here, $\varepsilon_{0i}(\varepsilon)$ are all branches inverse to the function $\varepsilon(\varepsilon_0) = \varepsilon_0 + U(\sqrt{m_p} l_1/\sqrt{2\varepsilon_0})$, and

$$f_\varepsilon(\varepsilon_0) = \frac{\exp\left[-\sqrt{\varepsilon_0/\langle\varepsilon\rangle}\right]}{2\sqrt{\varepsilon_0 \langle\varepsilon\rangle}}. \tag{4}$$

The latter is the initial distribution function of protons normalized to unity, which are emitted from the first target.[13] Here $\langle\varepsilon\rangle$ is the average energy of protons emitted from first target. The smooth initial energetic distribution (4) corresponds to the accelerated protons from the first target, containing hydrogen in their entire thickness.[8,9] For targets covered at the rear side with a thin layer of hydrogen or for ultrathin targets (tens of nm), one can expect a quasi- monochromatic distribution.[10,11] For such a case, one has to make use of following distribution:

$$f_\varepsilon(\varepsilon_0) = \frac{1}{\delta\varepsilon\sqrt{\pi}} \exp\left[-\frac{(\varepsilon_0 - \langle\varepsilon\rangle)^2}{\delta\varepsilon^2}\right], \tag{5}$$

which transforms in the limit $\delta\varepsilon \to 0$ to a monochromatic spectra, investigated above in the simulation.

Now, one has to develop the initial distribution function of the protons for the case of their transition through an accelerating "triangular" field. Such a situation occurs with thick targets or at the rear side of a target with moderate thickness when a prepulse is used, which creates a smooth density profile at the front side. For the accelerating triangular field function $\varepsilon(\varepsilon_0)$ determining the proton distribution, the temporal dependence of the potential (2) has a characteristic non-monotonic shape as it is shown in Fig. 4(a).

Correspondingly, as visible in Fig. 4, the inverse function shows in a specific energy interval three branches within a band, which is depicted by the blue lines. In the intervals below the green line (see Fig. 4), the energies ε, ε_0, and the distribution function are equal to the initial one. The green

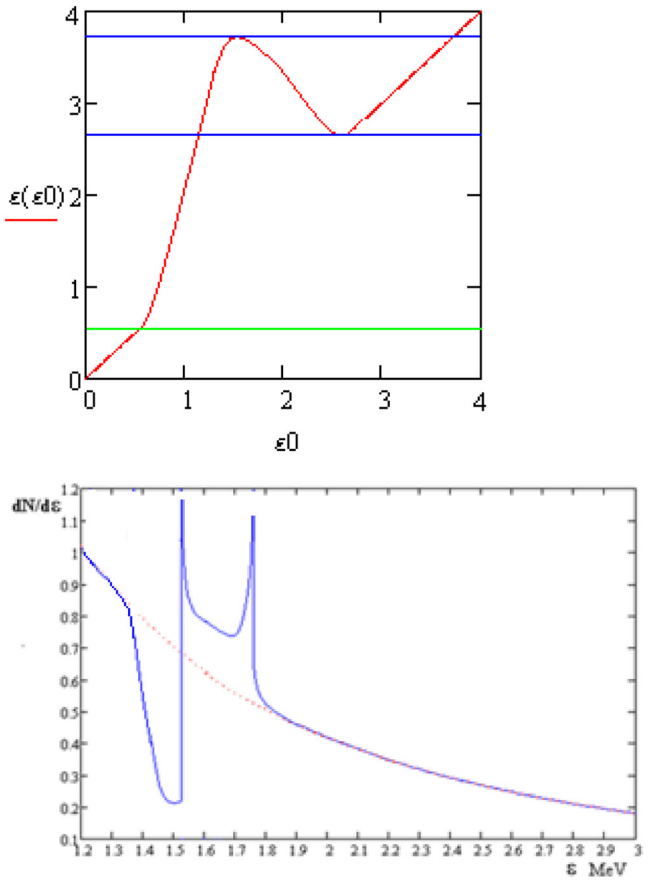

FIG. 4. (a) Function $\varepsilon(\varepsilon_0)$ for the accelerating triangular field; (b) distribution function of protons with smooth distribution function (red lines) after transition through the accelerating field. Calculation parameters are: $l_1 = 5\,\mu$m, $\varepsilon_{12} = 1.5$ MeV, $T_{eh2} = 0.3$ MeV, $\tau_f = 200$ fs, and $\nu = 10^{-3}$.

line originates at an energy ε, which is determined by equating the time of the proton motion between the two targets with the time of the field decay: $\sqrt{m_p} l_1/\sqrt{2\varepsilon_0(\varepsilon)} \approx t_{12} + \tau_f$ (protons with low energy will not be subjected by a field action). In the interval between the green line and the lower blue line $d\varepsilon_0/d\varepsilon < 1$, a dip is formed in the energy distribution, because the nominator in (3) exceeds the value 1 in the interval and diminishes the value of the distribution function.

The lower blue line is located at the energy of the local minimum in Fig. 4(a) and can be found from equation $\varepsilon'(\varepsilon_0) = 0$, $\varepsilon'' > 0$. When the energy arrives at the lower blue line, an ambiguity (2 branches) appears in the energy dependence $\varepsilon(\varepsilon_0)$. At the lower blue line in Fig. 4(a), the derivation is $\varepsilon'(\varepsilon_0) = 0$, $\varepsilon'' > 0$ and the distribution function becomes formally infinite (but can be integrated). In this case, a sharp high peak grows from the bottom of the dip (see Fig. 4(b)). In the interval between blue lines, the distribution function is the sum of the three branches. Finally, at the upper blue line, where again $\varepsilon'(\varepsilon_0) = 0$, $\varepsilon'' < 0$, the distribution function also has a sharp and high peak and on its right side the function goes back into the initial one. The appearance of the specific structure of the distribution function, i.e., the peaks, is connected with the non-stationary field: remaining particles fall in a stronger field and catch up with the leading protons. A multi-stream flow is created, which leads to vortices and an ambiguity of the proton energy distribution. In this case, the distribution function can be developed as follows: at the beginning, a parametrically given distribution function will be defined as

$$f_\varepsilon(\varepsilon_0) = \sum_i \frac{\exp\left[-\sqrt{\varepsilon_0/\langle\varepsilon\rangle}\right]}{2\sqrt{\varepsilon_0\langle\varepsilon\rangle}} \Bigg/ \sqrt{\left(\frac{\partial\varepsilon(\varepsilon_0)}{\partial\varepsilon_0}\right)^2 + \nu^2}\Bigg|_{\varepsilon_0=\varepsilon_{0i}(\varepsilon)} \tag{6}$$

with $\varepsilon(\varepsilon_0) = \varepsilon_0 + U(\sqrt{m_p} l_1/\sqrt{2\varepsilon_0})$. A parameter $\nu \ll 1$ is introduced in order to take away the singularities of the distribution function in the point, where $\varepsilon'(\varepsilon_0) = 0$. The number of particles at $\nu \ll 1$ does not depend on ν. The physical parameter ν comes from dissipative forces in the equation of motion of the proton. In the region of ambiguity of the dependence of $\varepsilon_0(\varepsilon)$ (see Figure 4(a)), the distribution (6) also has an ambiguity (3-branches) and therefore the distribution function has to be summed up over all branches. In order to sum up, one must consider the question of how to normalize the distribution (6). When ambiguity is absent, it is true that $\int_0^\infty f_\varepsilon(\varepsilon_0) d\varepsilon_0 = 1$, but in case of an ambiguity, this normalization can be only applied if the sign of the root in (6) coincides with those of the derivative $\varepsilon'(\varepsilon_0)$ and of the sum of the branches. At a negative root in (3, 6), one of the branches of the distribution also becomes negative, i.e., it becomes the case that $\delta\varepsilon(\varepsilon_0)/\delta\varepsilon_0 < 0$ (see also Fig. 4(a)). When joining the three branches of the distribution, one obtains in Fig. 4(b) the initial structure of the distribution function for protons propagating through the accelerating field. Particles, which create the peaks in Fig. 4(b), are launched in the region of the dip, whereby the total number of particles is conserved. For $\nu = 0$, the peaks in the distribution function have an infinite amplitude, but the particle number in them is limited. For calculation of the positions of the peaks and the dip in Fig. 4(a), an analytical formula was defined: for this purpose, we replaced the delay time t_{12} by the delay energy $\varepsilon_{I2} = m_p(l_1/t_{12})^2/2$. Then, it follows from formula (6) that the dip in the distribution function is formed at an energy ε_{12} (energy at the middle of the dip); thus, the position of the two peaks is determined by the two root expression a_1, a_2 in Eq. (7) as

$$\left[1 + \left(\alpha - \tilde{\varepsilon}_{12}{}^{-1/2}\right)^n \beta_{a,f}{}^n\right]^2 + \frac{n\beta_{a,f}{}^n}{2}\alpha^3\left(\alpha - \tilde{\varepsilon}_{12}{}^{-1/2}\right)^{n-1} = 0 \tag{7}$$

with $\alpha = \sqrt{T_{e2}/\varepsilon_0}$, $\beta_{a,f} = l_1\sqrt{m_p}/\tau_{a,f}\sqrt{2T_{e2}}$, $\tilde{\varepsilon}_{12} = \varepsilon_{12}/T_{e2}$.

Parameters a_1, a_2 determine the two energies ε_{01} and ε_{02} at which the parametrically default distribution function (6) has a maximum. For $n = 2$, the expression (7) is an equation of the 4th order. An approximate solution can be obtained for $\beta_{a,f} \gg 1$, $\beta_f > \beta_a$, and the peak energy can be than determined as $\varepsilon_{1,2} = \frac{T_{e2}}{\alpha_{1,2}{}^2} + U(T_{e2}/\alpha_{1,2}{}^2)\varepsilon_I$

$$\varepsilon_1 \approx \varepsilon_{12} + \frac{\varepsilon_{12}}{3\beta_f{}^{1/3}}, \quad \varepsilon_2 \approx \varepsilon_{12} + \frac{\varepsilon_{12}\sqrt{3}}{\beta_f{}^{1/3}}. \tag{8}$$

The distance between peaks $\varepsilon_2 - \varepsilon_1 \approx \frac{1.4\varepsilon_{12}}{\beta_f{}^{1/3}}$ enlarges with increasing laser intensity and duration. The particle number moving from the dip in the region of the peaks is

$$\delta N = \frac{0.5\sqrt{\varepsilon_{12}}\exp\left[-\sqrt{\varepsilon_{12}/\langle\varepsilon\rangle}\right]}{{\beta_f}^{1/3}\sqrt{\langle\varepsilon\rangle}}. \quad (9)$$

For targets of moderate thickness, the accelerating and the retarding triangles are nearly equal. When changing the sign of the field in (6) (retarding field), the peaks in Fig. 4(b) pass from the right side of the dip to the left side. The field, which is composed of the accelerating and the retarding triangles, creates the peaks at the right side as well as at the left side.

In the experiments,[6] tilted targets (45°), irradiated with p-polarized Gaussian laser pulses, with a spot diameter of 6 μm, a duration of 50 fs and an intensity of $I_L = 10^{19}$ W/cm^2 were investigated. The Ti targets of 1 μm thickness were polluted with a layer of hydrogen due to water adsorption. At a distance of 5 mm behind the Ti target, an Al target was positioned (corresponding to Fig. 1), which was irradiated at the rear side by a second laser pulse with the same parameters, but with a delay of 0.29 ns (delay energy $\varepsilon_{12} = 1.5$ MeV).

The character of the measured spectra in Ref. 6 corresponds to the spectra in Fig. 4(b), which resulted from the analytical model with parameters as given in the caption of Fig. 4. In the experimental spectra, the dip was located at the energy of 1.4 MeV (this corresponds to the experimental value of the parameter ε_{12} in the analytical model), whereas the peaks of the accelerated protons were located at 1.5 MeV and 1.6 MeV, respectively. The position of the dip in Fig. 4(b) at 1.5 MeV corresponds well to the experimental energy of the delay energy 1.5 MeV and to the dip position at 1.4 MeV in the experimental spectra. The dimensionless parameter $\beta_f = l_1\sqrt{m_p}/\tau_f\sqrt{2T_{e2}}$, which determines according to formula (8) the distribution peak, is at about $\beta_f \approx 530$ at the temperature of the hot electrons of $T_{e2} = m_e c^2(\sqrt{1 + I_L\lambda_L{}^2/1.37\,10^{18}\,(W\,\mu\text{m}^2/\text{cm}^2)} - 1) \approx 0.7$ MeV and a lifetime of the field at the target surface of $\tau_f \approx 800\,fs$ (calculations gave a lower value because of the simulation time limit). When putting the experimental parameters ε_{12}, β_f into formula (8), the calculated energy of the peaks in Fig. 4(b) is $\varepsilon_1 = 1.51$ MeV and $\varepsilon_2 = 1.77$ MeV, which is in good agreement with the measured values.

Acceleration of a proton bunch with one "triangular" field

Now, we consider an initial distribution (5) and an accelerating triangular field that is built up either at the front surface of a thick target or at the rear side of a μm-thick target in case of a laser prepulse. At $\delta\varepsilon < \varepsilon_{12}/{\beta_f}^{1/3}$ (with an enhancement of τ_f, it is also possible to fulfil this inequality at $\delta\varepsilon \sim \langle\varepsilon\rangle \sim \varepsilon_{12}$), a displacement of the whole Gaussian distribution function (5) takes place without changing its shape. The final distribution looks like

$$f_\varepsilon(\varepsilon) = \frac{1}{\delta\varepsilon\sqrt{\pi}}\exp\left[-\frac{\left(\varepsilon - \langle\varepsilon\rangle - U\left(\sqrt{m_p}l_1/\sqrt{2\langle\varepsilon\rangle}\right)\right)^2}{\delta\varepsilon^2}\right], \quad (10)$$

where $U(t)$ is given by the expression (2) with positive sign. In order to investigate the acceleration of protons with a broad energy spectra $\delta\varepsilon \gg \varepsilon_{12}/{\beta_f}^{1/3}$, one has to create the final distribution function for a subsequently enhanced duration of the field action τ_f. As delayed energy is chosen $\varepsilon_{12} = \langle\varepsilon\rangle$, this means that the main part of protons arrives to the second target in the moment of the maximal ambipolar field. Figs. 5(a) and 5(b) shows the evolution of the Gaussian distribution function as β_f is reduced.

At large β_f, only a part of the proton distribution will be accelerated, as seen in Fig. 5(a). The number of accelerated protons (right peak in Fig. 5(a)) in relation to the total proton number can be estimated as

$$\frac{\delta N}{N} \sim \frac{2(\tau_f + \tau_a)}{l_1}\sqrt{\frac{2\langle\varepsilon\rangle}{m_p}}\frac{\langle\varepsilon\rangle}{\delta\varepsilon}. \quad (11)$$

A reduction of β_f increases the number of accelerated protons and produces also the high peak in the distribution function. The energy broadening of the accelerated protons, in this case, can be smaller as the width of the initial distribution function (see Fig. 5(b)). At a further reduction of β_f as compared to Fig. 5(b), the peak in the figure converts into a

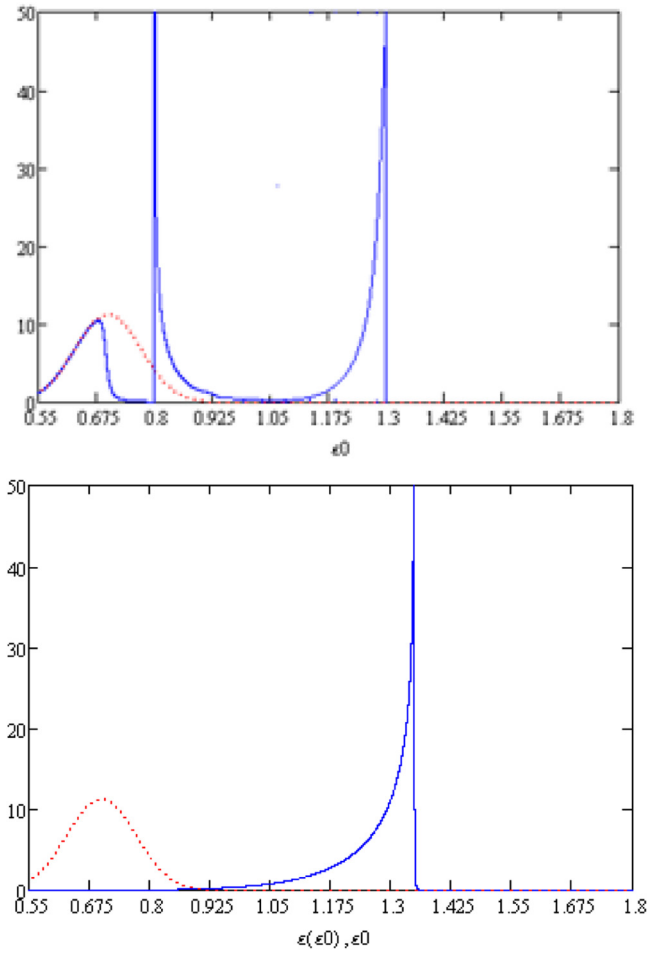

FIG. 5. Distribution functions of protons in accelerating field. The red dot line—initial distribution function, the blue solid line—distribution function after interaction. Here, the electron temperature of the second target is 60% of the first one. (a) Parameter $\beta_f = 15$—field with short lifetime and (b) $\beta_f = 5.3$—optimal field duration.

Gaussian distribution (10) and its width coincides with the initial one. A modification of the distribution function is in this case connected with an up-shift of the energy from the initial distribution. The optimal case for the acceleration process is shown in Fig. 5(b). Here, the maximal number of protons has a maximal energy and the energetic broadening is reduced in comparison to the initial distribution function (red line in Fig. 5(b)). In the following, the optimisation of the process is discussed in more details.

OPTIMIZATION OF THE ACCELERATION PROCESS

Let us determine optimum conditions for the post-acceleration of a Gaussian proton bunch with an energy $\langle\varepsilon\rangle$ and a dispersion $\delta\varepsilon$, in order to obtain a proton bunch of maximal energy and minimal energetic broadening. For an initial beam with small energetic broadening $\delta\varepsilon \ll \langle\varepsilon\rangle$, the time of the propagation from the first target to the second one is given by $t = \sqrt{m_p} l_1/\sqrt{2\langle\varepsilon\rangle}$. Correspondingly, the proton energy after the acceleration in the electric field (2) is $\varepsilon = \langle\varepsilon\rangle + U(\sqrt{m_p} l_1/\sqrt{2\langle\varepsilon\rangle})$. The maximum value ε is realized, when the energy of the delay is $\varepsilon_{21} = \langle\varepsilon\rangle$ (or, if $t = t_{21}$, what is the same, see (2)) and $U = T_{e2}$. In this case, all the protons of the initial distribution enter the accelerating field in the moment of its maximum and their final energy is $\varepsilon = \langle\varepsilon\rangle + T_{e2}$. The electron temperature of the second target can be chosen (by laser intensity) from the condition that the protons arrive at the given energy value ε. In case of limited width of the initial distribution $\delta\varepsilon \le \langle\varepsilon\rangle$, the maximal energy of the accelerated peak of the distribution function is $\varepsilon \le \langle\varepsilon\rangle + T_{e2} + \delta\varepsilon$. An estimation of the maximal energy of the distribution peak in dependence of $\delta\varepsilon/\langle\varepsilon\rangle$, ε_{12} can be made according to formula (4) and leads only to a small difference from the version for a small initial distribution

$$\frac{\varepsilon}{\langle\varepsilon\rangle} \approx 1 + \frac{T_{e2}}{\langle\varepsilon\rangle} + 0.2\frac{\delta\varepsilon}{\langle\varepsilon\rangle}. \tag{12}$$

Expression (8) determines also the position of the right-hand peak (ε_2), but at an arbitrary value of the acceleration parameter. If putting in (8), the optimal delay energy $\varepsilon_{12} = \langle\varepsilon\rangle$ and the optimal parameter β_f, the expressions (8) and (12) correspond to each other when taking into account that (8) was derived for the distribution (5) with an effective $\delta\varepsilon \approx \langle\varepsilon\rangle$.

It is known that TNSA acceleration is depending on the intensity as $T_{e2}(I_2) \sim I_2{}^{\mu}$, where $\mu \sim 0.5$.[12] In this case, the coefficient of energy enhancement for the two targets of equal structure is given by

$$\frac{\varepsilon}{\langle\varepsilon\rangle} \approx 1 + \left(\frac{I_2}{I_1}\right)^{\mu} + 0.2\frac{\delta\varepsilon}{\langle\varepsilon\rangle}. \tag{13}$$

Here, $I_{1,2}$ is the laser intensity at the first and second targets (pulse duration is assumed to be of equal value). It is worth to note that if the two pulses are combined into one and if directed on only one target instead of two, the proton energy is enhanced by factor $\varepsilon/\langle\varepsilon\rangle = (1 + I_2/I_1)^{\mu}$. Therefore, the use of two targets is beneficial if intensities $I_{1,2}$ are comparable. If $I_2 \gg I_1$ (or $\mu \to 1$), the difference in the acceleration is only small. In this case, the advantage of such two-target system consists in a "compression" of the energy distribution, i.e., in the generation of a quasi-monochromatic beam. As shown in Figure 6 is the dependence of the relative enhancement of the proton energy on the intensity ratio I_2/I_1 at the acceleration in case of two targets and for only one target. In our simulation of the post-acceleration of the proton bunch, no first laser pulse was assumed and instead of it a proton bunch with given energy was taken initially. A monoenergetic proton distribution can be obtained when laser pulse is interacting with an ultrathin plastic target[11] or with a double-layered target, where an ultrathin layer of hydrogen is located at the rear side.[9] The paper[12] was given the expression (6), which allows combine laser intensity and duration with the proton energy and there is also pointed out that there is an optimal target thickness in order to reach this energy. The proton of energy 10 MeV is possible to produce with 100 nm-thick carbon target, which is covered with 10 nm hydrogen and irradiated by a 50 fs laser pulse with intensity of $I_1 = 4 \times 10^{19}$ W/cm^2. According to the simulation, the proton energy increases in this case due to the second laser pulse (with intensity 3.4×10^{19} W/cm^2 and 50 fs duration) from 10 MeV to 22 MeV. In Figure 6, these values are shown with black squares, located close to the solid black line resulting from the formula (13).

At a given T_{e2}, the number of protons with maximal energy ε depends on the width of the initial distribution, duration of the accelerating field and the distance between the two targets. In the case of a nearly monochromatic initial distribution, i.e., at $\delta\varepsilon/\langle\varepsilon\rangle \ll 1$, the condition for the life time of the field and the distance between the targets for optimal acceleration is fulfilled by the inequality

$$\frac{\delta\varepsilon}{\langle\varepsilon\rangle} < \frac{2(\tau_f + \tau_a)}{l_1}\sqrt{\frac{2\langle\varepsilon\rangle}{m_p}}, \tag{14}$$

which represents the condition that during the life time of the field, all protons of Gaussian distribution have

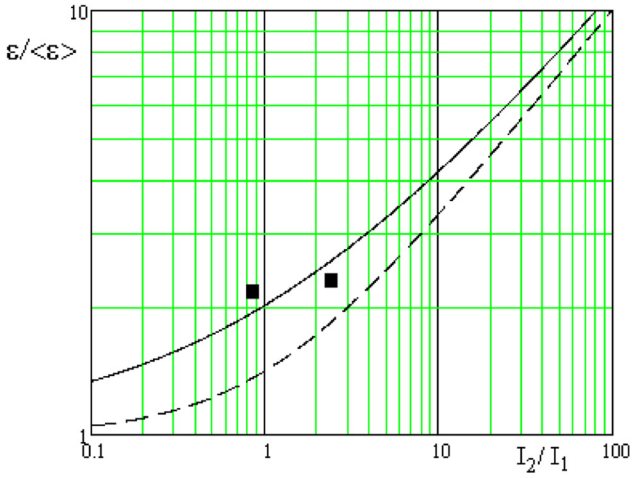

FIG. 6. The coefficient of energy enhancement $\varepsilon/\langle\varepsilon\rangle$ of the proton bunch at optimal acceleration as function of the laser intensity ratio at the first and second targets (solid line). Dotted line shows the energy enhancement for the case of mutual irradiation of these pulses on only one target. Two black squares are the results of the simulations of the accelerated protons having a distribution according to Figs. 2(a) and 8.

propagated through the field. In the paper,[7] this condition was not mentioned, because there it was obviously assumed that it is automatically fulfilled for a mono-energetic proton distribution. The distribution function of protons has, in this case, the form of Eq. (10) and the energy broadening $\delta\varepsilon$ remains at the level of the initial distribution.

The inequality (14) corresponds to the case of very small values of the dimensionless parameter $\beta_f < 1$. However, expression (14) for a broad energetic distribution is not optimal, because, in this case, the distribution can be reduced at the acceleration. Such reduction behaviour is illustrated in Fig. 5(b), showing the transformation of a Gaussian distribution into a narrow peak. The optimal variant takes place if $\beta_f = \beta_f{}^*$, which depends on the ratios $\delta\varepsilon/\langle\varepsilon\rangle$ and $T_{e2}/\langle\varepsilon\rangle$. The condition is fulfilled, if the parameter $\varepsilon(\varepsilon_0) = \varepsilon_0 + U(\sqrt{m_p}l_1/\sqrt{2\varepsilon_0})$ has an extremum. At this extreme point $\varepsilon_0{}^*$, the value of $\varepsilon(\varepsilon_0)$ has to be close to the averaged energy value $|\varepsilon_0{}^* - \langle\varepsilon\rangle| < \delta\varepsilon$. The condition of the appearance of one extremum in the dependence $\varepsilon(\varepsilon_0)$ is mathematically equivalent to the second root of Eq. (10). Because an analytical solution of Eq. (11) is complicated, we are using the simulation results for the dependence of the optimal $\beta_f{}^*$ on the parameters.

Figure 7(a) shows that for sufficiently broad distributions, the optimal value of β_f no longer depends on the distribution width. It is worth noting that the enhancement in Fig. 7(a) in the region of small values of the ratio $\delta\varepsilon/\langle\varepsilon\rangle$ is connected with the condition of maximal compression of the initial distribution. However, for small $\delta\varepsilon/\langle\varepsilon\rangle$, such a compression is not specifically required, once the distribution is already close to a monoenergetic one. The use of an asymptotic value β_f^* for narrow distributions results in a conservation of their width and their Gaussian shape and therefore one can state that for proton energy enhancement, the optimal parameter is β_f^*, which does not depend on $\delta\varepsilon/\langle\varepsilon\rangle$. A broad distribution will be, in this case, accelerated and compressed, whereas a narrow distribution is only accelerated. Such values β_f^* for an energy enhancement of protons are displayed in Fig. 7(b). From Figures 6 and 7, one can take the optimal parameters of the second laser pulse and second target for the certain energy enhancement factor. Specifically, Fig. 6 allows a determination of the relative intensity for such a case and Fig. 7 gives the distance between the two targets in order to involve the entire distribution in the acceleration process.

In order to test this double-target method, simulations were performed to accelerate a quasi- monoenergetic proton bunch with $\varepsilon_0 = 80\,\text{MeV}$, $\delta\varepsilon = 10\,\text{KeV}$ up to an energy of 200 MeV. Generation of 80 MeV protons is now experimentally available as published in Ref. 1 and also in detail described in the theoretical paper[12] for the case of very thin carbon targets of 240 nm thickness, covered on the rear side with 30 nm hydrogen and irradiated with a 50 fs laser pulse of intensity $I_1 = 4\times10^{20}\,\text{W/cm}^2$. The laser intensity at the second target should be in this case of $10^{21}\,\text{W/cm}^2$ in accordance to the expression (13). In our model, the spatial distribution of the protons in the propagation direction (positive x-coordinate) in front of the second target is connected with the energy width at their generation region in the first target:

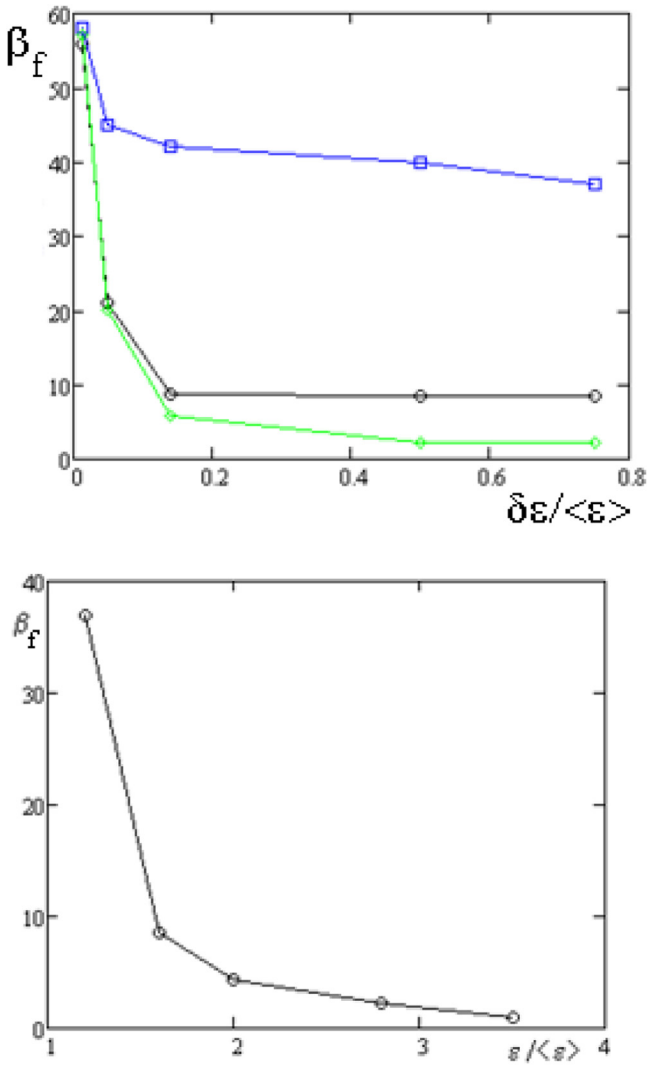

FIG. 7. (a) Optimal value of parameter β_f as function of $\delta\varepsilon/\langle\varepsilon\rangle$ and $T_{e2}/\langle\varepsilon\rangle = 0.2$ (blue line), 0.6 (black line), and 1.8 (green line). (b) Dependence of optimal value of β_f on the normalized energy enhancement.

$\delta x = \delta\varepsilon\, l_1/2\langle\varepsilon\rangle$. In the simulation, a quasi-monochromatic distribution is used, but the longitudinal extension needs an additional evaluation. As in the analytical model, all protons of the bunch have in the optimal case to interact with the field during its lifetime: $\delta x < \tau_f\sqrt{2\varepsilon_0/m_p}$. Starting from this condition and the thickness of the second target, the longitudinal and the transversal size of the proton bunch were chosen as $0.5\mu\text{m}\times2\mu\text{m}$ and a Gaussian profile over the full simulation was assumed. The target was taken to be a 6 μm thick Al^{+6} layer with ion density of 10 n_{cr}, longitudinal size of 6 μm, and a transversal one of 8 μm. A target of such density and size can be produced by a laser prepulse, preceding the second pulse. The limitation of the transversal parameter was introduced in order to prevent both a dispersion of the electron cloud and an enhancement of the electron temperature. So as to eliminate a slow-down of the protons at the front surface of the second target, the initial position (given by the delay time) of the centre of the proton bunch was chosen to be inside of the Al target at the distance of 1 μm from the front side. A laser pulse of $10^{21}\,\text{W/cm}^2$, 40 fs, with a diameter of 6 μm irradiated the front surface simultaneously

with the start of the motion of the proton bunch with $n_p = 0.05\, n_{cr}$. During the motion of the proton bunch to the rear surface (40 fs), the entire laser pulse can interact with the target.

In Fig. 8, the distribution function at the moment 100 fs after the start of the laser pulse is displayed. It is visible that the electrons captured by the proton bunch have broadened the width of the distribution by ~12% (for the main part of the distribution). Additionally, it is identifiable that a small part of protons have arrived at energy of 210 MeV, which is connected to the acceleration process of the bunch within the Al target caused by hot electrons. The enhancement factor of the energy in this simulation was 2.3. Corresponding to Fig. 6 for such enhancement the two-step scheme is better in comparison with the use of only one target. Fig. 6 shows that the black square of the performed simulation is close to the analytical curve. This underlines the potential of a cascaded energy enhancement of a proton bunch in the energy range highly interesting for important applications.

The analytical model developed and the resulting optimal acceleration parameters are assuming that any feedback of the proton bunch on the field at the second target is missing, i.e., the protons can be seen as probe particles. In the appendix, the limitation for the proton density is given for which our approach is valid. Optimization of the dense bunch parameters and the corresponding modelling requires additional investigations, which is out of the scope of this work. For the evaluation of the acceleration efficiency of proton bunches of various densities we have, following the simulation results, looked for the dependence of the proton numbers contained in a 5% energy range near the distribution function cut-off on the initial proton bunch density for different initial proton energies. Simulation has shown that the number of protons of this group decreases as well with the enhancement of the bunch density as with the increase of its initial energy. Specifically, such decrease takes place also when the total number in the proton bunch at a density of $n_{\mathbf{cr}}$ is increased by a factor of 20. That means that to create a maximal number of protons in a small energy range the best choice is an acceleration of a proton bunch with low density and low initial energy.

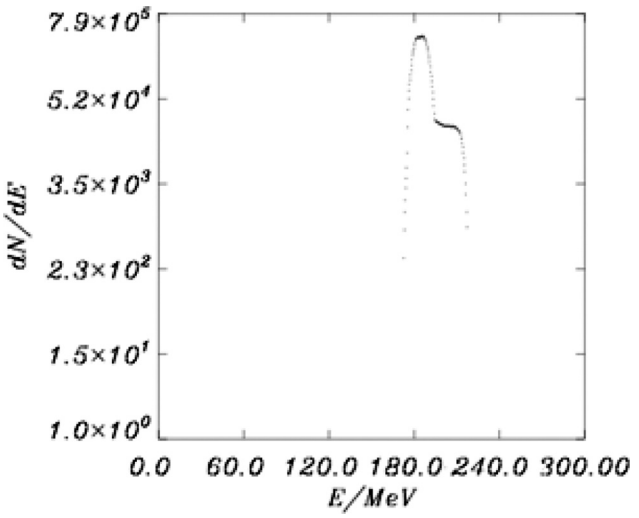

FIG. 8. Distribution function of protons in case of the acceleration of 80 MeV mono-energetic bunch by the factor of 2.5. Laser pulse with an intensity 10^{21} W/cm^2, duration 40 fs, and 6 μm diameter irradiates Al^{+6} target with ion density of 10 n_{cr}, and thickness of 5 μm in which the proton bunch with density $n_p = 0.05\, n_{cr}$ moves.

SUMMARY

It is shown that a cascaded scheme is very favourable for proton acceleration with lasers using two or more targets and correspondingly also laser pulses irradiating the targets one after the others with a given delay. Such an acceleration scheme is more efficient (delivers higher proton energy) at optimized parameters compared to the case of combined laser pulses in one and its interaction with only one target. An additional advantage of a cascaded system is the option to create a nearly mono-energetic proton spectrum ("compression" of the distribution function). In the result, a cascaded system makes it possible to generate protons with energies of several hundreds of MeV, specifically required for medical applications, with laser systems of reduced power, which are much cheaper and easier to operate. The highest efficiency can be obtained, if the laser pulses have a comparable intensity at each of the cascade targets. In this case, the proton energy is maximized as compared to the case with two combined pulses into one irradiating only one target. Vice versa, at a remarkable difference in the intensities of the laser pulses, the cascaded scheme loses its advantage and practically the same proton energy can be obtained with two combined pulses and one target (which is experimentally easier to set up). With aid of the analytical model, the optimization of the parameters of such a cascaded acceleration scheme was performed and the optimal distance between two targets, the delay time between the two laser pulses and even the parameters of the pulses to obtain certain proton energy were evaluated. The analytical model and the resulting optimal parameters of the cascaded system are usable for proton bunches with a density, which is less than the density of the hot electrons in the target of the second or following cascades. The analytical calculation was proven with help of 2D PIC simulations of the acceleration and propagation of the proton bunch in the laser target.

ACKNOWLEDGMENTS

A.A.A. acknowledges the provided computation resources of JSC at the Project HBU15.

APPENDIX

The distribution function of the accelerated protons (6) is now developed under the assumption of a single-particle character of the interaction of the proton with the accelerating field. In the following, the maximal density of the proton bunch will be determined up to which this approach can be used. The optimal value of parameter $\beta_f{}^*$ allows to determine an optimal spatial bunch length L_p just before its entrance into the acceleration region: $L_p = \beta_f{}^* \sqrt{\frac{2T_{eh2}}{m_i}} \tau_f \frac{\delta\varepsilon}{\langle\varepsilon\rangle}$. This length L_p is much larger than the initial bunch length L_{p0} at its creation area at the rear side of the first target. The proton

layer determined by the thickness of the absorbing surface of the metallic target is of several tens of nanometers with a density of n_{p0}, comparable with solid density. Accordingly, the length L_{p0} is between tens of nanometers up to several tenths part of a micron. In the considered MeV range of the proton energy L_p is about one micron. The density of the proton bunch decreases on the way between first and second targets up to the value

$$n_p = \frac{n_{p0}L_{p0}}{\beta_f * \sqrt{\frac{2T_{eh2}}{m_i}}\tau_f \frac{\delta\varepsilon}{\langle\varepsilon\rangle}}. \quad \text{(A1)}$$

Here, $n_{p0}L_{p0}$ is the number of protons in units of the transversal area of the bunch. In the process of the bunch acceleration, the hot electrons created in the second target propagate in vacuum together with the bunch forming such quasi-neutral plasma with an electron concentration $n_{ehp} \approx n_p$. The existence of hot electrons in the acceleration region of the proton bunch results in the appearance of an electric field $E_p \approx \sqrt{T_{eh2}n_p}$ at this region. This field is additionally accelerating protons at the right-hand boundary of the bunch and slows them down at the left-hand one at its further propagation. In the model, given here, this field is not taken into account but obviously it leads to a broadening of the peak in the distribution function of the protons as shown in Figs. 5 and 7. This broadening is visible in the experimental distribution in Ref. 6 as compared to the calculated one of Fig. 4(b). However, the parameter v (see (8)) introduced in our model enables to take quantitatively into account such broadening. To neglect the field E_p as compared to the field $E \approx \sqrt{T_{eh2}n_{eh}}$ at the rear side of the second target, a small concentration of the proton bunch in comparison with the concentration of the hot electrons at the second target is required. Assuming that the duration time of the fields E and E_p is of the same order of magnitude ($\sim\tau_f$) and evaluating the change in the velocity of the proton motion under the action of the field as $eE\tau_f$, one can obtain the limitation for the density of the proton bunch, at which the broadening in the proton energy due to the field E_p does not exceed the given value $\Delta\varepsilon/\varepsilon$:

$$\frac{n_p}{n_{eh}} \le \frac{\Delta\varepsilon}{\varepsilon}. \quad \text{(A2)}$$

Expressions (A1) and (A2) can be seen as conditions for the application of the above described model and as requirement to generate a "monoenergetic" proton spectra in the cascaded acceleration. It is worth to note that for targets of micron thickness, the hot electron density n_{eh} is of about the tenth part of the critical density n_{cr}. Therefore, the proton density n_p is of about percents of the critical density for the case of $\Delta\varepsilon/\varepsilon \sim 0.1$. Thereby, the initial density of the proton bunch can be about L_p/L_{p0} times higher. From the model, it follows that quasi-monoenergetic proton bunches in case of an additional acceleration in a second target are only possible, if the proton density in the beam is low enough, i.e., $n_p < n_{eh}$.

[1]I. J. Kim, K. H. Pae, C. M. Kim, H. T. Kim, J. H. Sung, S. K. Lee, T. J. Yu, I. W. Choi, C.-L. Lee, K. H. Nam, P. V. Nickles, T. M. Jeong, and J. Lee, Phys. Rev. Lett. **111**, 165003 (2013).
[2]S. V. Bulanov, T. Z. Esirkepov, V. S. Khoroshkov, A. V. Kuznetsov, and F. Pegoraro, Phys. Lett. A **299**, 240 (2002).
[3]I. Velchev, E. Fourkal, and C.-M. Ma, Phys. Plasmas **14**, 033106 (2007).
[4]E. Fourkal, C. M. Ma, and I. Velchev, J. Plasma Phys. **75**, 235 (2009).
[5]S. M. Pfotenhauer, O. Jackel, J. Polz, S. Steinke, H. P. Schlenvoigt, J. Heymann, A. P. L. Robinson, and M. C. Kaluza, New J. Phys. **12**, 103009 (2010); T. Kluge, W. Enghardt, S. D. Kraft, U. Schramm, Y. Sentoku, K. Zeil, T. E. Cowan, R. Sauerbrey, and M. Bussmann, Phys. Rev. E **82**, 016405 (2010).
[6]F. Abicht, M. Schnürer, J. Bränzel, G. Priebe, A. A. Andreev, C. Koschitzki, S. Steinke, T. Toncian, O. Willi, and W. Sandner, Proc. SPIE **8779**, 87790V-1 (2013).
[7]W. P. Wang, B. F. Shen, X. M. Zhang, X. F. Wang, J. C. Xu, X. Y. Zhao, Y. H. Yu, L. Q. Yi, Y. Shi, L. G. Zhang, T. J. Xu, and Z. Z. Xuet, Phys. Plasmas **20**, 113107 (2013).
[8]P. Mora, Phys. Plasmas **12**, 112102 (2005).
[9]H. Daido, M. Nishiuchi, and A. Pirozhkov, Rep. Prog. Phys. **75**, 056401 (2012).
[10]A. A. Andreev, S. Steinke, M. Schnurer, P. V. Nickles, and K. Y. Platonov, Phys. Plasmas **17**, 123111 (2010).
[11]S. Steinke, A. Henig, M. Schnürer, T. Sokollik, P. Nickles, D. Jung, D. Kiefer, R. Hörlein, J. Schreiber, T. Tajima, X. Q. Yan, M. Hegelich, J. Meyer-ter-Vehn, W. Sandner, and D. Habs, Laser Part. Beams **28**, 215 (2010).
[12]A. Andreev and K. Y. Platonov, Opt. Spectrosc. **111**, 191 (2011).
[13]A. V. Gurevich, L. V. Pariiskay, and L. P. Pitaevskii, Sov. Phys. JETP **22**, 449 (1966).
[14]D. Neely, P. Foster, and A. Robinson, Appl. Phys. Lett. **89**, 021502 (2006).